



## Optimal Selection of Cutting Parameters for Surface Roughness in Milling Machining of AA6061-T6

K. Danesh Narooei<sup>a</sup>, R. Ramli<sup>b</sup>

<sup>a</sup> Department of Industrial Engineering, Faculty of Industry and Mine Khash, University of Sistan and Baluchestan, Zahedan, Iran

<sup>b</sup> Department of Mechanical and Manufacturing Engineering, Faculty of Engineering and Built Environment, Universiti Kebangsaan Malaysia, Malaysia

### PAPER INFO

#### Paper history:

Received 11 September 2021

Received in revised form 03 March 2022

Accepted 06 March 2022

#### Keywords:

Milling Machining

Surface Roughness

AA6061-T6

Cutting Parameters

### ABSTRACT

Due to its ability to remove material quickly while maintaining optimum surface quality, end milling is considered one of the most frequent metal cutting procedures in industry. The present study aimed to investigate the impacts of cutting parameters and tool geometry on milling of Aluminum Alloy 6061-T6 to examine the impact surface roughness by utilizing response surface methodology (RSM). RSM was used to create a second-order mathematical model of surface roughness for this purpose. A multiple regression analysis used the analysis of variance to demonstrate the effect of machining settings on surface roughness and determine experiment performance. The trials for optimizing surface roughness were set up utilizing the central composite design (CCD) method and various cutting parameters such as spindle speed, feed rate and depth of cut. Also the parameters used in tool geometry are the radial rake angle (10, 13, 16, 19 and 22 degrees), and nose radius (0, 0.2, 0.4, 0.6 and 0.8 mm). The result shows that the nose radius has more significant effect on the surface roughness followed by the radial rake angle. Moreover, the effect of the depth of cut on surface roughness is more dominant than cutting speed. The optimum combinations of cutting and tool geometry parameters were cutting speed (60.53 m/min), feed rate (0.025 mm/tooth), depth of cut (0.84 mm), radial rake angle (12.72 degree) and nose radius (0.34 mm).

doi: 10.5829/ije.2022.35.06c.08

## 1. INTRODUCTION

The oldest process to shape components is metal cutting or machining in the manufacturing industry [1]. It is evaluated that 15% of the all-mechanical part produced worldwide is derived from machining operation. Metal cutting is a general term applied to a group of processes that includes material removal and shaping process to generate parts with various methods [2]. Material removal is desirable necessary in manufacturing operation for multiple reasons such as dimensional accuracy, high surface finish, and sharp corners and flatness [3]. The machining process can produce a variety of shapes and parts. The machining operation can be defined as a system including workpiece, cutting tool and the machine. The interactions among these elements are necessary to determine an efficient and economical

machining process [4,5]. The general machining process are turning, milling, boring, drilling, planning, shaping, broaching, and sawing [6]. One of the common machining processes is milling to produce complicated parts in the various industries [7,8].

In the last decade, the metal cutting process continued to grow significantly with time to obtain optimum machining process efficiency. The offering optimum machining parameters is often the primary factor in attaining this specific purpose to develop along with implement a high effective procedure control intended for machining operations through parameter optimization [9]. The cutting process is affected by several factors such as tool geometry, cutting parameters, temperature and tool wear. The tool geometry parameters have high influence when compared by other factors on the quality of surface product [10,11].

\*Corresponding  
(K. Danesh Narooei)

Author: [kh\\_dnarooei@eng.usb.ac.ir](mailto:kh_dnarooei@eng.usb.ac.ir)

The milling process is capable of producing a variety of configuration with the utilized different milling cutter. The basic types of milling cutters with common milling operation are slab milling, face milling and end milling [10]. In milling process the main goal is to produce the parts with high quality in minimum machining time. In minimizing the machining time, the researcher utilized various optimization methods to determine the optimum airtime motion. The optimization method employed to determine the minimum distance between each node. The quality and machining time in milling process may be affected by various cutting conditions and tool geometry. The cutting conditions are feed rate, cutting speed, axial depth of cut and radial depth of cut. The main tools of geometry are radial rake angle, nose radius, helix angle, radial relief angle and axial relief angle [12] as shown in Figure 1. These parameters play a significant role in success of aforementioned matters in machining.

The qualities of machining, production rate and operational cost are the main three objectives in machining application. These three objectives are conflicting objectives for the machining process. Setting up effective machining parameters and appropriate airtime motion has been an issue for industrial companies for approximately a century and is still the focus of several studies. Obtaining optimal cutting conditions is a major challenge in the manufacturing industry, where the economy of machining operations is critical in a competitive market. In terms of improving machining quality, dimensional accuracy and surface roughness are mentioned [13, 14]. The effectiveness of the machining process and the optimal surface roughness are always dependent on selecting the proper cutting conditions [15, 16]. This cutting condition is divided into two parts: cutting parameters and tool geometry. Cutting parameters are cutting speed, feed rate and cutting depth of cut [17, 18]. Nose radius, helix angle and radial rake angle are considered the three most important tool geometries parameters.

Given the importance of the milling operation in contemporary manufacturing industries, it is required to improve machining quality and minimize machining time

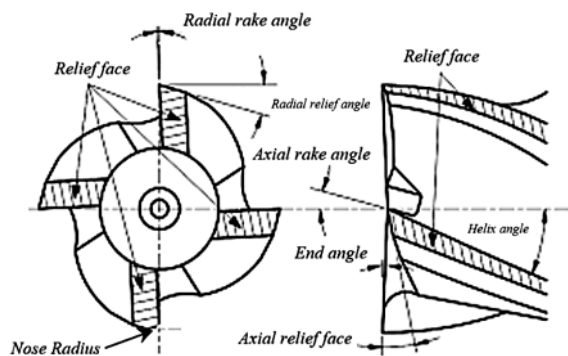


Figure 1. Tool geometry definition

for such an operation. However, an attempt has been made in this work to investigate the effect of tool geometry (nose radius and radial rake angle) and cutting parameters (feed rate, cutting speed, and depth of cut) on the surface quality achieved during the end milling process.

A functional series of advantageous statistical and mathematical methods that are successfully employed to model and optimize the issues and problem related to the engineering field is called RSM. RSM is a technique whose major aim is to enhance and optimize the obtained responses which were affected by different factors related to the input process [19]. Besides, the connections between received responses and the factors related to manageable input are quantified by RSM. RSM has some significant practical functions. Among the applications assigned to the RSM, the ones in new products designing, improving and organizing as well as in the existing product designing and improving can be mentioned [20]. Independent variables work in isolation or in combination. These variables cause some influences that affect the processes. Here, RSM clarifies these effects on the processes created by the independent variables. When manufacturing processes need to be modelled and optimized by RSM technique, enough data and information is gathered using planned experimentation.

## 2. MATERIALS AND METHODS

### 2. 1. Materials

Aluminium is the third most abundant element in the earth's crust, as well as the second most consumed metal by weight, trailing only iron and its alloys [21]. Modern aluminum alloys are useful for structural applications and as steel replacements to their low density and attractive features such as high ductility and corrosion resistance. Table 1 shows the commercial designations of many aluminum alloys, together with their principal alloying elements and applications in industry.

T temper is further classified into ten conditions. T6, which has been solution treated and artificially aged, is one of the most frequent tempers [22]. Magnesium and silicon are components of the aluminum alloy-T6. Aluminium alloy-T6 has medium strength, good machinability, formability, and weldability, as well as high corrosion resistance. The chemical properties of AA 6061-T6 are summarized in Tables 1.

### 2. 2. Preparation

The experiment were designed based on five factors feed rate, cutting speed, depth of cut, nose radius and radial rake angle in five factor levels as listed in Table 2. These five levels for each cutting condition selected from literature review determined by previous researcher as mentioned as optimum range of cutting conditions. These five factors in five levels

**TABLE 1.** Chemical composition of AA 6061-T6

Component	Weight, %
Silicon	0.8
Iron	0.7
Copper	0.4
Manganese	0.15
Magnesium	1.2
Chromium	0.35
Zinc	0.25
Titanium	0.15
Other elements	0.15
Remainder Aluminium	95.85

selected to design experiment for surface roughness test by central composite design method (CCD). The experiments were performed on AA 6061-T6 using high speed steel end mill cutter based on central composite design containing of 32 coded value as summarized in Table 3. The Minitab 19.1.1 software version 2019 was utilized to arrange the experimental design and analyses the results obtained.

**2. 3. Characterization** After the finished milling machining process according to the experimental design, the  $R_a$  arithmetic surface roughness was adopted and measured on the machined surface roughness. The measurements were taken after finished all the 32 experiments with surface roughness tester Mitutoyo SV-C3100W4 as shown on Figure 2. Averaging surface

**TABLE 2.** Process parameters and their levels

Parameters	Symbol	Unit	Factor levels				
			-2	-1	0	1	2
Cutting speed	N	m/min	31.4	39.25	47.1	54.95	62.8
Feed rate	F	mm/tooth	0.025	0.03	0.035	0.04	0.045
Depth of cut	D	mm	0.4	0.6	0.8	1	1.2
Radial rake angle	$\alpha$	degree	10	13	16	19	22
Nose radius	r	mm	0	0.2	0.4	0.6	0.8

**TABLE 3.** Experimental design for central composite design in coded value

Run	Coded value				
	N	F	D	$\alpha$	r
1	-1	-1	-1	-1	1
2	1	-1	-1	-1	-1
3	-1	1	-1	-1	-1
4	1	1	-1	-1	1
5	-1	-1	1	-1	-1
6	1	-1	1	-1	1
7	-1	1	1	-1	1
8	1	1	1	-1	-1
9	-1	-1	-1	1	-1
10	1	-1	-1	1	1
11	-1	1	-1	1	1
12	1	1	-1	1	-1
13	-1	-1	1	1	1
14	1	-1	1	1	-1
15	-1	1	1	1	-1
16	1	1	1	1	1

17	-2	0	0	0	0
18	2	0	0	0	0
19	0	-2	0	0	0
20	0	2	0	0	0
21	0	0	-2	0	0
22	0	0	2	0	0
23	0	0	0	-2	0
24	0	0	0	2	0
25	0	0	0	0	-2
26	0	0	0	0	2
27	0	0	0	0	0
28	0	0	0	0	0
29	0	0	0	0	0
30	0	0	0	0	0
31	0	0	0	0	0
32	0	0	0	0	0

roughness values at sites located (D1, D2, and D3) on the cutting path of the workpiece generated the  $R_a$  values of the machined surface roughness. Figure 3 illustrated the

surface roughness experiment and measured region for surface roughness test. The failure criterion for the surface roughness experiment was kept at  $6 \mu\text{m}$ .

For the prediction of  $R_a$ , a second-order polynomial response is designed. Finally, ANOVA is used to assess the model's appropriateness. The optimization methods' objective function results in the lowest value of  $R_a$ .

### 3. RESULTS

$R_a$  was evaluated in the dry milling process of AA 6061-T6 using HSS tool under various cutting parameters. The surface roughness predicted model developed based on five response cutting parameters, which are N, F, D,  $\alpha$  and r. The milling process in the dry machining process utilized for this experiment. All constant parameters selected from the data handbook. The parametric study and design optimization were performed utilized RSM in the design of the experiment statistical methods. This method is simple to use and provides a thorough review of the factors that influence a specific response.

The experiment is carried out to collect the required data, and regression analysis is utilized to generate a realistic surface roughness prediction model. Table 4 shows the design matrix with the results of completed



Figure 2. Surface roughness tester Mitutoyo SV-C3100W4

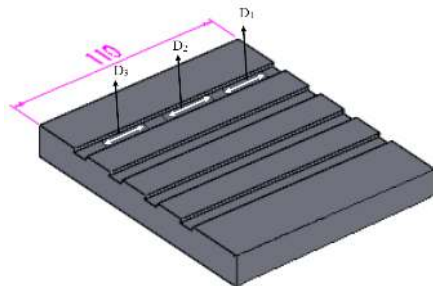


Figure 3. The surface roughness experiment in milling process

TABLE 4. Design matrix and results for surface roughness

Run	Coded value					Response Surface roughness
	N	F	D	$\alpha$	r	$R_a$
1	-1	-1	-1	-1	1	1.66
2	1	-1	-1	-1	-1	1.74
3	-1	1	-1	-1	-1	2.69
4	1	1	-1	-1	1	1.95
5	-1	-1	1	-1	-1	2.92
6	1	-1	1	-1	1	2.50
7	-1	1	1	-1	1	2.20
8	1	1	1	-1	-1	3.13
9	-1	-1	-1	1	-1	3.01
10	1	-1	-1	1	1	2.44
11	-1	1	-1	1	1	2.36
12	1	1	-1	1	-1	3.30
13	-1	-1	1	1	1	2.27
14	1	-1	1	1	-1	3.28
15	-1	1	1	1	-1	3.33
16	1	1	1	1	1	2.06
17	-2	0	0	0	0	2.79
18	2	0	0	0	0	2.83
19	0	-2	0	0	0	3.31
20	0	2	0	0	0	3.58
21	0	0	-2	0	0	3.46
22	0	0	2	0	0	4.07
23	0	0	0	-2	0	1.16
24	0	0	0	2	0	2.04
25	0	0	0	0	-2	2.75
26	0	0	0	0	2	1.34
27	0	0	0	0	0	3.11
28	0	0	0	0	0	3.07
29	0	0	0	0	0	3.03
30	0	0	0	0	0	2.88
31	0	0	0	0	0	3.27
32	0	0	0	0	0	3.25

surface roughness. The minimum and maximum surface roughness were  $1.16 \mu\text{m}$  and  $3.58 \mu\text{m}$  for runs 23 and 20, respectively. The minimum surface roughness determined by combination of cutting conditions N ( $47.1 \text{ m/min}$ ), F ( $0.025 \text{ mm/tooth}$ ), D ( $0.8 \text{ mm}$ ), and tool geometry r ( $0.4 \text{ mm}$ ) and  $\alpha$  ( $10 \text{ degree}$ ).

In this research, the MINITAB software is employed to analyze and generate a prediction mathematical model. The analysis of variance (ANOVA) of statistical analysis results of  $R_a$  is shown in Table 5. In Table 5, the F and P values from the model are 52.42 and  $<0.0001$ , respectively; indicates that the selected model is significant. The other p-values higher than 0.05 implies the model terms are insignificant. In this case, N, the interaction of the cutting condition and tool geometry, NF, ND,  $N\alpha$  and interaction of the Nr are insignificant. These five effects have p-values of higher than 0.05, which means that they are insignificant for a confidence level of 95%. The ANOVA table shows the linear, square and interaction components. The linear, square and

interaction components are significant with small p-values. Also, the  $R^2$  with 98.96% and Adj  $R^2$  with 97.07% are shown the other adequacy of the experiment.

The large p-value 0.9021 compared to the pure error indicates that the model does not effectively fit the response surface. In addition, Table 5 demonstrates that the  $\alpha$  and r have the greatest influence on surface roughness, with F-values of 77.08 and 235.96, respectively. Furthermore, with a P-value of 0.9444 and greater than 0.05, N is negligible.

$R^2$  statistic indicates that the fitted second-order model accounts for 98.96 percent of variability in surface roughness by the independent variables. For model adequacy; they were checking utilized normal. They used normal probability and residual versus predicted graphs to test model adequacy.

Figure 4, the normal probability plot of the standardized residuals demonstrates that the errors from the  $R_a$  model are normally distributed, since the points on the plot are pretty close to the straight line. It can be used to ensure that the basic assumptions underlying the analysis are met. Figure 5 demonstrates that the residuals for a specific location in standardized residuals vs.

TABLE 5. ANOVA table for surface roughness test

Source	Sum-of-Square	DF	Mean-square	F-Ratio	P-value
Model	14.29	20	0.71	52.42	$<0.0001$
N	6.943E-005	1	6.943E-005	5.093E-003	0.9444
F	0.13	1	0.13	9.41	0.0107
D	0.59	1	0.59	43.32	$<0.0001$
$\alpha$	1.05	1	1.05	77.08	$<0.0001$
r	3.22	1	3.22	235.96	$<0.0001$
N*N	3.595E-003	1	3.595E-003	0.26	0.6177
F*F	0.019	1	0.019	1.40	0.2620
D*D	4.076E-003	1	4.076E-003	0.30	0.5954
$\alpha*\alpha$	0.059	1	0.059	4.33	0.0615
r*r	0.18	1	0.18	13.05	0.0041
N*F	0.074	1	0.074	5.46	0.0394
N*D	0.20	1	0.20	15.01	0.0026
N* $\alpha$	0.52	1	0.52	37.83	$<0.0001$
N*r	0.11	1	0.11	7.84	0.0173
F*D	0.16	1	0.16	11.78	0.0056
F* $\alpha$	0.24	1	0.24	17.34	0.0016
F*r	0.14	1	0.14	10.26	0.0084
D* $\alpha$	0.66	1	0.66	48.32	$<0.0001$
D*r	4.52	1	4.52	331.31	$<0.0001$
$\alpha*r$	2.31	1	2.31	169.11	$<0.0001$
Residual	0.15	11	0.014		
Lack of Fit	0.041	6	6.907E-003	0.32	0.9021
Pure Error	0.11	5	0.022		
Cor Total	14.44	31			$<0.0001$

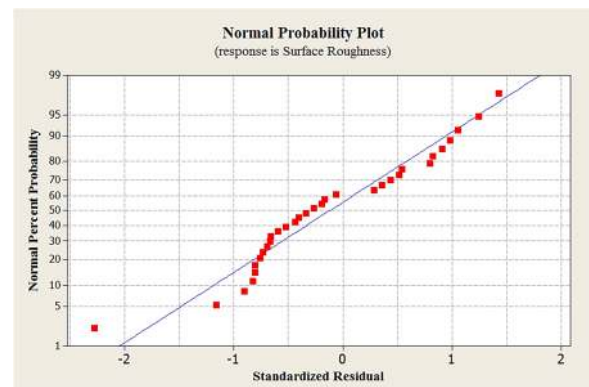


Figure 4. Normal probabilities of residuals for surface roughness

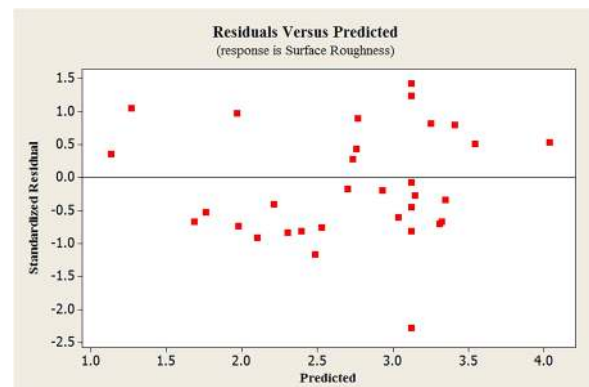


Figure 5. The plot of residuals versus predicted response for surface roughness

expected values of  $R_a$  are fairly distributed, and the plot revealed no obvious patterns or distinctive structures. As a result, it is possible to conclude that the suggested model is adequate.

Therefore, according to the previous definition, can confidently generate the predicted mathematical model. It can be utilized to perform the parametric study from the model and response optimization. The predicted mathematical model of the surface roughness generated by RSM as shown by Equation (1).

$$\begin{aligned}
 R_a = & -19.0651 + 0.00164844 N + 0.00692201 F + 2.4234 D \\
 & + 1.87551 \alpha + 9.65229 r - 0.00000359095 N^2 \\
 & + 0.000027617 F^2 + 3.74607 D^2 - 0.043598 \alpha^2 \\
 & - 7.00831 r^2 - 0.00000559955 NF + 0.000345113 ND \\
 & + 0.0000106408 N\alpha + 0.000607637 Nr - 0.0105439 FD \\
 & - 0.000454575 F\alpha - 0.0113086 Fr - 0.299227 D\alpha \\
 & - 2.04341 Dr - 0.166981 \alpha r
 \end{aligned} \quad (1)$$

where  $R_a$  indicates the surface roughness in  $\mu\text{m}$ ,  $N$  represents the cutting speed (m/min),  $F$  shows the feed rate (mm/tooth),  $D$  is the depth of cut (mm),  $\alpha$  shows the radial rake angle (degree), and  $r$  is the nose radius (mm). Equation 1 can be used to estimate the influence of the chosen cutting parameters on surface roughness and to determine the best range of values.

The three-dimensional surface plots were used to determine the effect of the cutting parameter on  $R_a$ . Based on a model equation, these charts explain how a response variable interacts with the two components. Additionally, these graphs can be used to determine ideal response values and design circumstances. Figure 6 depicts the surface plot's interaction effect on  $N$  and  $D$  on  $R_a$ . This graph indicates that the faster the  $N$ , the lower the  $R_a$ . The curve has a steeper upward slope in the side to the  $D$ , according to this plot. However, the  $D$  has a wide range of effects on  $R_a$ . To establish the minimal  $R_a$ , it is important to keep the  $D$  at a lower value and the  $N$  at a greater value. These trends are similar to the finding of Reddy and Rao [23] and Kumar et al. [24]. The surface plot of the effect of  $\alpha$  and  $N$  on  $R_a$  as shown in Figure 7. As shown in this figure, the curve has a greater upward slope on the  $\alpha$  side and a slight curvature on the  $N$  side. The quadratic terms in the  $N$  and  $\alpha$  directions cause the curvatures in the  $N$  and  $\alpha$  directions, respectively. This appears to determine the minimal  $R_a$ ; the  $\alpha$  must be maintained at lower levels. These trends are similar to the finding of Maheshesh et al. [15].

The interaction effects on the  $r$  and  $N$  on the  $R_a$  are depicted on a surface plot as shown in Figure 8. In the side of the  $r$  appeared convex curve from lower for higher values. According to surface plot, the  $N$  increases from 31.4 to 62.8 m/min has an insignificant effect of the  $R_a$ . As shown, the minimum  $R_a$  was produced at lower and higher values of  $r$  of the higher value of  $N$ . These trends are similar to the finding of Reddy and Rao [23].

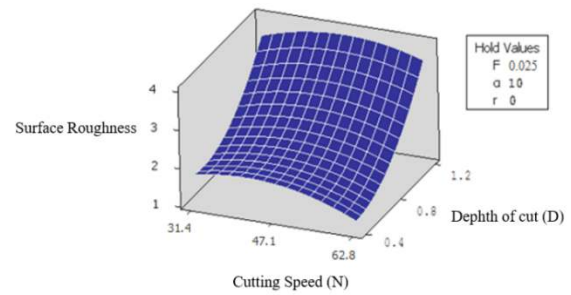


**Figure 6.** The three-dimensional surface of the surface roughness against  $N$  and  $D$

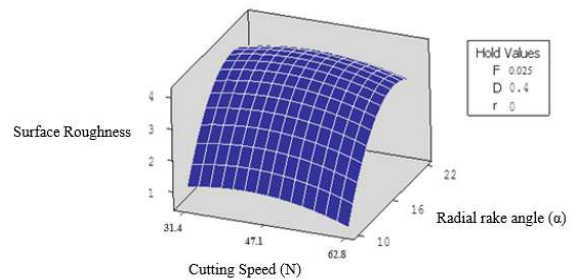


**Figure 7.** The three-dimensional surface of the surface roughness against  $N$  and  $\alpha$

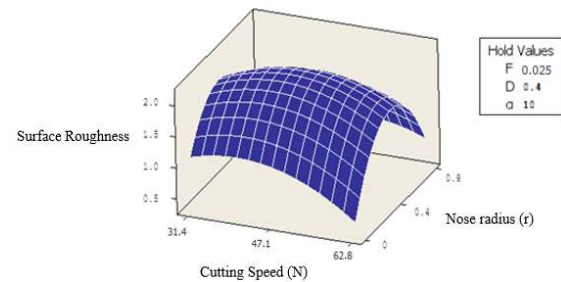


**Figure 8.** The three-dimensional surface of the surface roughness against  $N$  and  $r$

The interaction impact of  $\alpha$  and  $D$  on  $R_a$  is depicted in Figure 9. The minimal  $R_a$  calculated for lower  $\alpha$  and  $D$  values. As shown, the variation in  $\alpha$  has considerable different effects on  $R_a$  at lower values at the  $D$ . The curvature on the  $\alpha$  side demonstrates that a change in this value reduces the  $R_a$  quality. In addition, increasing the  $D$  value decreases the  $R_a$  quality on the side to the  $D$  values. These trends are similar to the finding of Raja and Baskar [25].

The interaction effect of  $D$  and  $r$  on  $R_a$  is shown on Figure 10. The curve shows the curvature from the  $r$  side view while it shows the steeper upward curve from the  $D$  side view. Considering the  $D$  effects, as can be seen, the  $R_a$  quality decreases as the  $D$  increase. This trend is similar to the finding of Li et al. [26]. The three-dimensional surface of the  $R_a$  in a micrometer against to the two cutting parameter's  $\alpha$  and  $r$  are shown in Figures 11. The curve is shows the convex curvature from the  $r$



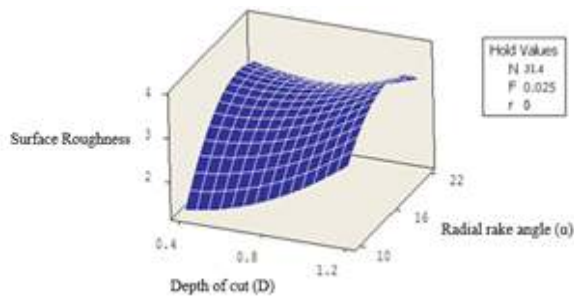


**Figure 9.** The three-dimensional surface of the surface roughness against D and  $\alpha$

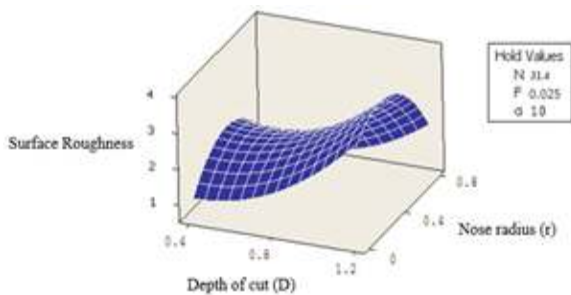


**Figure 10.** The three-dimensional surface of the surface roughness against D and r

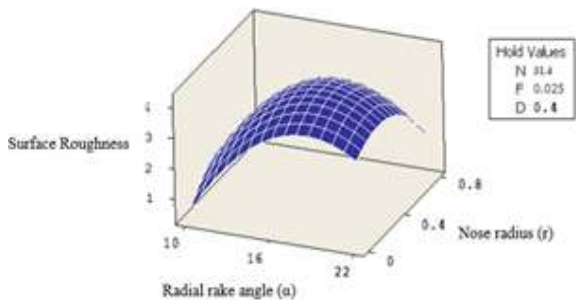


**Figure 11.** The three dimensional surface of the surface roughness against  $\alpha$  and r

side view while it shows the steeper upward curve from the D. As shown, increasing the  $\alpha$  has a significant diverse effect of the  $R_a$  with a peak at about 16 degrees. Then the  $R_a$  quality starts to increase in  $3 \mu\text{m}$  on the r of 22 mm. In the side of r, the convex curvature shows the optimum  $R_a$  determined as lower and higher r values. These trends are similar to the finding of Maheshesh et al. [15] and Zain et al. [27].

#### 4. CONCLUSION

In this research, the optimization of  $R_a$  under the various cutting parameters in the dry milling process on AA 6061-T6 has been investigated. An investigation of the cutting parameters which are N, D, F, r and  $\alpha$ , it is found

that the r has a more significant effect on the  $R_a$  followed by  $\alpha$ .  $R_a$  is least affected by N. It was observed that the  $R_a$  increased at the F,  $\alpha$  and D increased. Moreover, the  $R_a$  was decreased as the N increased. In the r parameters, the  $R_a$  has minimum values on lower and higher values of the r factors. The minimum  $R_a$  determined by combination of cutting condition N (47.1 m/min), F (0.025 mm/tooth), D (0.8 mm) and in tool geometry, r (0.4 mm) and  $\alpha$  (10 degree).

#### 5. REFERENCES

- Zhuang, K., Fu, C., Weng, J., Hu, C. "Cutting edge microgeometries in metal cutting: a review." *The International Journal of Advanced Manufacturing Technology*, Vol. 116, No. 7, (2021), 2045-2092. <https://doi.org/10.1007/s00170-021-07558-6>
- Li, S., Sui, J., Ding, F., Wu, S., Chen, W., Wang, C. "Optimization of Milling Aluminum Alloy 6061-T6 using Modified Johnson-Cook Model" *Simulation Modelling Practice and Theory*, Vol. 111, (2021), 102330. <https://doi.org/10.1016/j.simpat.2021.102330>
- Jawahir, I., Brinksmeier, E., M'saoubi, R., Aspinwall, D., Outeiro, J., Meyer, D., Umbrello, D., Jayal, A. "Surface integrity in material removal processes: Recent advances" *CIRP Annals-Manufacturing Technology*, Vol. 60, No. 2, (2011), 603-626. <https://doi.org/10.1016/j.cirp.2011.05.002>
- Kim, Y. M., Shin, S. J., Cho, H. W. "Predictive modeling for machining power based on multi-source transfer learning in metal cutting" *International Journal of Precision Engineering and Manufacturing-Green Technology*, Vol. 9, No. 1, (2022), 107-125. <https://doi.org/10.1007/s40684-021-00327-6>
- Saighneh, A., Hajjalimohammadi, A., Abedini, V. "Cutting Forces and Tool Wear Investigation for Face Milling of Bimetallic Composite Parts Made of Aluminum and Cast Iron Alloys" *International Journal of Engineering, Transactions C: Aspects*, Vol. 33, No. 6, (2020), 1142-1148. DOI: 10.5829/ije.2020.33.06c.12
- Zhu, K. "Modeling of the Machining Process", In *Smart Machining Systems* Springer, Cham., (2022), 19-70, DOI: 10.1007/978-3-030-87878-8\_2
- Kant, T., Pare, V. "Study of optimum process selection parameter in high speed cnc end milling of composite materials using meta heuristic optimization" *International Journal of Science & Technology*, Vol. 1, No. 2, (2022), 9-18.
- Prasanth, I. S. N. V. R., Ravishankar, D. V., Manzoor Hussain M., "Analysis of Milling Process Parameters and their Influence on Glass Fiber Reinforced Polymer Composites (RESEARCH NOTE)" *International Journal of Engineering, Transactions A: Basics*, Vol. 30, No. 7, (2017), 1074-1080 DOI: 10.5829/ije.2017.30.07a.17
- Zailani, Z. A., Rusli, N. S. N., Shuaib, N. A., "Effect of Cutting Environment and Swept Angle Selection in Milling Operation" *International Journal of Engineering, Transactions C: Aspects*, Vol. 34, No. 11, (2021), 2578-2584 DOI: 10.5829/ije.2021.34.11bc.02
- Gao, X., Cheng, X., Ling, S., Zheng, G., Li, Y., Liu, H. "Research on optimization of micro-milling process for curved thin wall structure" *Precision Engineering*, Vol. 73, (2022), 296-312. <https://doi.org/10.1016/j.precisioneng.2021.09.015>
- Venkata Vishnu, A., Sudhakar Babu, S., "Mathematical Modeling and Multi Response Optimization for Improving Machinability of

- Alloy Steel using RSM, Grey Relational Analysis and Jaya Algorithm" *International Journal of Engineering, Transactions C: Aspects*, Vol. 34, No. 09, (2021), 2157-2166. DOI: 10.5829/IJE.2021.34.09C.13
12. Reddy, N. S. K., Rao, P. V. "Selection of optimum tool geometry and cutting conditions using a surface roughness prediction model for end milling", *The International Journal of Advanced Manufacturing Technology*, Vol. 26, No. (11-12), (2005), 1202-1210. <https://doi.org/10.1007/s00170-004-2110-y>
  13. Esfandiari, A. "Cuckoo Optimization Algorithm in Cutting Conditions During Machining" *Journal of Advances in Computer Research* Vol. 5, No. 2, (2014), 45-57.
  14. Hassan, A., El-Hamid, A., Wagih, A., Fathy, A. "Effect of mechanical milling on the morphology and structural evaluation of Al-Al<sub>2</sub>O<sub>3</sub> nanocomposite powders" *International Journal of Engineering, Transactions A: Basics*, Vol. 27, No. 4, (2014), 625-632. DOI: 10.5829/idosi.ije.2014.27.04a.14
  15. Mahesh, G., Muthu, S., Devadasan, S. "Prediction of surface roughness of end milling operation using genetic algorithm" *The International Journal of Advanced Manufacturing Technology* Vol. 77, No. (1-4), (2015), 369-381. <https://doi.org/10.1007/s00170-014-6425-z>
  16. Nakhaei, M. R., Naderi, G. "Modeling and Optimization of Mechanical Properties of PA6/NBR/Graphene Nanocomposite Using Central Composite Design" *International Journal of Engineering, Transactions C: Aspects*, Vol.33, No. 9, (2020), 1803-1810. DOI: 10.5829/ije.2020.33.09c.15
  17. Lauro, C. H., Pereira, R. B., Brandão, L. C., Davim, J. P. "Design of Experiments—Statistical and artificial intelligence analysis for the improvement of machining processes: A review" *Design of Experiments in Production Engineering*, (2016), 89-107. DOI: 10.1007/978-3-319-23838-8\_3
  18. Edem, I. F., Balogun, V. A. "Energy efficiency analyses of toolpaths in a pocket milling process" *International Journal of Engineering, Transactions B: Application*, Vol. 31, No. 5, (2018), 847-855. DOI: 10.5829/ije.2018.31.05b.22
  19. Sahith Reddy, S., Achyutha Kumar Reddy, M. "Optimization of Calcined Bentonite Clay Utilization in Cement Mortar using Response Surface Methodology" *International Journal of Engineering, Transactions A: Basics* Vol. 34, No. 7, (2021), 1623-1631. DOI: 10.5829/ije.2021.34.07a.07
  20. Vahdani, M., Ghazavi, M., Roustaei, M. "Prediction of Mechanical Properties of Frozen Soils Using Response Surface Method: An Optimization Approach" *International Journal of Engineering, Transactions A: Basics* Vol. 33, No. 10, (2020), 1826-1841. DOI: 10.5829/ije.2020.33.10a.02
  21. Ozdemir, F., Witharamage, C. S., Darwish, A. A., Okuyucu, H., Gupta, R. K. "Corrosion behavior of age hardening aluminum alloys produced by high-energy ball milling" *Journal of Alloys and Compounds*, Vol. 900, (2022), 163488. <https://doi.org/10.1016/j.jallcom.2021.163488>
  22. Kadigama, K., Noor, M. M., Rahman, M. M., Rejab, M. R. M., Haron, C. H. C., Abou-El-Hossein, K. A. "Surface roughness prediction model of 6061-T6 aluminium alloy machining using statistical method" *European Journal of Scientific Research*, Vol. 25, No. 2, (2009): 250-256.
  23. Reddy, N. S. K., Rao, P. V. "Selection of an optimal parametric combination for achieving a better surface finish in dry milling using genetic algorithms." *The International Journal of Advanced Manufacturing Technology*, Vol. 28, No. (5-6), (2006): 463-473. <https://doi.org/10.1007/s00170-004-2381-3>
  24. Kumar, M. S., Prasad, J., Krishna, D. A., Narayana, M. V., Anusha, M., Saravanakumar, A. "Parametric optimization of aluminium alloy milling using Taguchi method for surface roughness" *International Journal of Scientific Research and Review*, Vol. 7, No. 3, (2018), 516-522.
  25. Raja, S. B., Baskar, N. "Application of particle swarm optimization technique for achieving desired milled surface roughness in minimum machining time" *Expert Systems with Applications* Vol. 39, No. 5, (2012), 5982-5989. <https://doi.org/10.1016/j.eswa.2011.11.110>
  26. Li, B., Tian, X., Zhang, M. "Modeling and multi-objective optimization of cutting parameters in the high-speed milling using RSM and improved TLBO algorithm" *The International Journal of Advanced Manufacturing Technology*, Vol. 111, No. 7, (2020), 2323-2335. <https://doi.org/10.1007/s00170-020-06284-9>
  27. Zain, A. M., Haron, H. Sharif, S. "Simulated annealing to estimate the optimal cutting conditions for minimizing surface roughness in end milling Ti-6Al-4V" *Machining Science and Technology*, Vol. 14, No. 1, (2010), 43-62. <https://doi.org/10.1080/10910340903586558>

---

### Persian Abstract

#### چکیده

فرآیند فرزکاری یکی از متداول ترین مراحل برش فلزات در صنعت است زیرا توانایی آن در حذف سریع مواد با کیفیت سطح مطلوب ثابت شده است. در این مقاله بر اساس روش سطح پاسخ (RSM) اثرات پارامترهای مختلف برشکاری و هندسه ابزار در فرزکاری بر زبری سطح مورد بررسی قرار گرفته است. در همین راستا یک مدل ریاضی مرتبه دوم از زبری سطح با استفاده از RSM توسعه داده شده است. همچنین تجزیه و تحلیل رگرسیون چندگانه با استفاده از تجزیه واریانس برای نشان دادن اثر پارامترهای ماشینکاری بر زبری سطح و تعیین عملکرد آزمایش انجام شده است. در بهینه سازی زبری سطح، آزمایش ها با استفاده از روش طراحی مرکب مرکزی (CCD) با استفاده از پارامترهای مختلف سرعت برش، نرخ پیشروی، عمق براده برداری انجام شده است. همچنین پارامترهای زاویه آزاد ابزار (۱۰، ۱۳، ۱۶، ۱۹ و ۲۲ درجه) و زاویه نوک ابزار (۰، ۰.۲، ۰.۴، ۰.۶ و ۰.۸ میلی متر) در هندسه ابزار مورد بررسی قرار گرفته است. نتیجه نشان می دهد که زاویه نوک ابزار و به دنبال آن زاویه آزاد ابزار تأثیر چشمگیری در زبری سطح دارد. علاوه بر این، تأثیر عمق براده برداری بر زبری سطح بیشتر از سرعت برش است. در نهایت ترکیب بهینه پارامترهای برش و هندسه ابزار، سرعت برش (۶۰.۵۳ متر در دقیقه)، نرخ پیشروی (۰.۰۲۵ میلی متر بر دندانه)، عمق براده برداری (۰.۸۴ میلی متر)، زاویه آزاد ابزار (۱۲.۷۲ درجه) و زاویه نوک ابزار (۰.۳۴ میلی متر) بدست آمده است.

---